ARTICLE OPEN

Check for updates

Dissecting biological heterogeneity in major depressive disorder based on neuroimaging subtypes with multi-omics data

Lili Tang[1,2,7], Rui Tang[1,2,7], Junjie Zheng[1,2], Pengfei Zhao[1,2], Rongxin Zhu[1,2], Yanqing Tang[3]✉, Xizhe Zhang[1,4]✉, Xiaohong Gong[5]✉ and Fei Wang[1,2,6]✉

The heterogeneity of Major Depressive Disorder (MDD) has been increasingly recognized, challenging traditional symptom-based diagnostics and the development of mechanism-targeted therapies. This study aims to identify neuroimaging-based MDD subtypes and dissect their predominant biological characteristics using multi-omics data. A total of 807 participants were included in this study, comprising 327 individuals with MDD and 480 healthy controls (HC). The amplitude of low-frequency fluctuations (ALFF), a functional neuroimaging feature, was extracted for each participant and used to identify MDD subtypes through machine learning clustering. Multi-omics data, including profiles of genetic, epigenetics, metabolomics, and pro-inflammatory cytokines, were obtained. Comparative analyses of multi-omics data were conducted between each MDD subtype and HC to explore the molecular underpinnings involved in each subtype. We identified three neuroimaging-based MDD subtypes, each characterized by unique ALFF pattern alterations compared to HC. Multi-omics analysis showed a strong genetic predisposition for Subtype 1, primarily enriched in neuronal development and synaptic regulation pathways. This subtype also exhibited the most severe depressive symptoms and cognitive decline compared to the other subtypes. Subtype 2 is characterized by immuno-inflammation dysregulation, supported by elevated IL-1 beta levels, altered epigenetic inflammatory measures, and differential metabolites correlated with IL-1 beta levels. No significant biological markers were identified for Subtype 3. Our results identify neuroimaging-based MDD subtypes and delineate the distinct biological features of each subtype. This provides a proof of concept for mechanism-targeted therapy in MDD, highlighting the importance of personalized treatment approaches based on neurobiological and molecular profiles.

Translational Psychiatry (2025)15:72 ; https://doi.org/10.1038/s41398-025-03286-7

INTRODUCTION

Over the last few decades, the recognition of Major Depressive Disorder (MDD) as a condition of inherent heterogeneity has posed significant challenges to the conventional diagnostic framework that relies on symptom clusters [1]. This heterogeneity is characterized by a significant mismatch between symptom dimensions and their biological underpinnings, where identical symptoms may arise from different biological causes, and disparate symptoms may reflect similar biological changes [2, 3]. Such discrepancies make it necessary to develop precise diagnostic and therapeutic strategies based on the disease's underlying mechanisms. Despite extensive efforts, the identification of reliable biomarkers for MDD diagnosis remains elusive. Furthermore, the prevalent trial-and-error approach in the current diagnostic system yields disappointing outcomes, with less than one-third of MDD patients experiencing remission after initial treatments [4–6]. About one-third of patients do not achieve clinical recovery even after undergoing 12-week courses of four distinct antidepressants over a year [7]. The intricate heterogeneity of MDD plays a significant role in these diagnostic and treatment dilemmas. Strategically redefining MDD into biologically homogeneous subtypes, guided by objective biomarkers, could pave the way for more accurate and effective precision diagnostics and treatments.

With the rapid advancement in biotechnologies, researches into MDD adopt multiple biological characteristics, including neuroimaging [8–10], electroencephalography (EEG) [11, 12], and multi-omics molecular profiles [13–15], to delineate biological subtypes. Neuroimaging stands out as a pivotal intermediate phenotype bridging the gap between etiology and behavioral manifestations [16, 17]. Studies have employed functional, structural, and diffusion tensor imaging to categorize MDD patients into subgroups with homogenous neuroimaging patterns [18, 19], providing significant insights into the categorization and

[1]Early Intervention Unit, Department of Psychiatry, The Affiliated Brain Hospital of Nanjing Medical University, Nanjing, China. [2]Functional Brain Imaging Institute of Nanjing Medical University, Nanjing, China. [3]Department of Psychiatry, Shengjing Hospital of China Medical University, Shenyang, China. [4]School of Biomedical Engineering and Informatics, Nanjing Medical University, Nanjing, China. [5]State Key Laboratory of Genetic Engineering, MOE key Laboratory of Contemporary Anthropology, School of Life Sciences, Fudan University, Shanghai, China. [6]Department of Psychiatry, School of Public Health, Nanjing Medical University, Nanjing, China. [7]These authors contributed equally: Lili Tang, Rui Tang. ✉email: tangyanqing@cmu.edu.cn; zhangxizhe@njmu.edu.cn; gongxh@fudan.edu.cn; fei.wang@yale.edu

Received: 3 August 2024 Revised: 22 December 2024 Accepted: 12 February 2025
Published online: 04 March 2025

therapeutic management of MDD. The Amplitude of Low-Frequency Fluctuations (ALFF) is a neuroimaging metric for measuring local spontaneous neuronal activity during rest. It has been validated for high test-retest reliability, establishing its utility as a regional functional measure to discern individual differences [20, 21]. In prior research, we observed alterations in the ALFF metric within specific brain areas, including the prefrontal cortex, occipital lobe, hippocampus, and amygdala of MDD patients, facilitating the delineation of subtypes in MDD [22, 23].

Despite prior studies having classified MDD into relatively homogeneous subtypes using neuroimaging features, limited researches have verified their underlying biological mechanisms at the multi-omics level. Most studies focused solely on comparing their symptomatology, or indirect verification through publicly available databases. It is noteworthy that existing etiological hypotheses, such as the monoamine hypothesis [24], polygenic hypothesis, immuno-inflammatory hypothesis [25], mitochondrial dysfunction [26], and metabolic dysregulation [27], offer diverse insights into the biological underpinnings of MDD. However, none of these hypotheses can fully explain the pathological mechanism of MDD [3], supporting the biological heterogeneity of MDD. Different subtypes may have stronger associations with particular etiological theories. Defining biologically homogeneous subtypes through neuroimaging characteristics and corroborating their biological relevance with omics data from the same neuroimaging cohort will help elucidate the leading etiological mechanisms of each subtype, offering vital directions for precision medicine of MDD.

This study aims to identify subtypes of MDD based on ALFF and investigate the biological underpinnings using multi-omics data. In the present study, we recruited 327 MDD patients and 480 healthy controls (HC) and clustered MDD patients into three subtypes based on ALFF patterns. Subsequently, we conducted comparative analyses across various molecular levels, including pro-inflammatory cytokine, epigenetics, metabolomics, and genetics profiles, to delineate the predominant molecular alterations of each subtype.

MATERIALS AND METHODS

Participants

A total of 807 participants were included in this study, including 327 MDD patients and 480 HC. Patients with MDD were recruited from both inpatient and outpatient services at the Department of Psychiatry within the First Affiliated Hospital of China Medical University and Shenyang Mental Health Center. HC were recruited through local community advertisements and had no personal or family history of psychiatric disorders. All participants were independently evaluated by two trained psychiatrists. For participants aged 18 years and older, the Structured Clinical Interview for Diagnostic and Statistical Manual of Mental Disorders, Fourth Edition (DSM-IV) Axis I Disorders was employed. Participants under 18 years old were diagnosed using the Schedule for Affective Disorders and Schizophrenia for School-Age Children-Present and Lifetime version (K-SADS-PL). Exclusion criteria for participation included: (1) general contraindications for MRI, (2) a history of substance or alcohol abuse/dependence (3) head trauma with loss of consciousness lasting at least 5 min or any neurological disorder, and (4) any major concurrent medical disorder, such as preexisting cardiac, inflammatory, and/or autoimmune illness. The study was approved by the Medical Research Ethics Committee of China Medical University in accordance with the Declaration of Helsinki. Written informed consent was received from each subject or their legal guardian for young participants under 18 years old.

Clinical assessment

The Hamilton Depression Scale (HAMD) and the Hamilton Anxiety Scale (HAMA) were used to evaluate the severity of depressive and anxiety symptoms in all participants. Cognitive function was assessed by a computerized version of the Wisconsin Card Sorting Test (WCST), which provides five indices as follows: correct responses (CR), completed categories (CC), total errors (TE), perseverative errors (PE), and non-perseverative errors (NPE).

Neuroimaging data acquisition and preprocessing

MRI scans were acquired with a 3.0 T GE Sigma system (Sigma EXCITE HDx, GE Healthcare, USA) with a standard 8-channel head coil at the First Affiliated Hospital of the China Medical University, Shenyang, China. A restraining foam pad was utilized to minimize head movement. Participants received explicit instructions to remain in a relaxed state, keep their eyes closed, and refrain from any movement or falling asleep throughout the scanning. The functional images were performed using a gradient echo planar imaging (EPI) sequence, which was as following parameters: repetition time = 2000 ms, echo time = 30 ms, flip angle = 90°, field of view = 240 × 240 mm^2, and matrix = 64 × 64. A total of 35 slices were acquired, each with a thickness/gap of 3 mm/0 mm. The scanning session lasted for 6 min and 40 s. The images underwent processing and analysis employing two toolkits: Statistical Parametric Mapping 8 (SPM8, http://www.fil.ion.ucl.ac.uk/spm) and Data Processing Assistant for R-functional MRI-fMRI (DPARSF, http://www.restfmri.net/forum/DPARSF). The specific parameters and processing of MRI data (Supplementary Methods S1) were consistent with our prior publications [28–30].

Identification of neuroimaging subtypes

The AAL90 atlas, a standard brain mask, was used to extract voxel-level ALFF values from the neuroimaging data, ensuring accurate mapping of these values to standardized brain regions for subsequent analysis. We utilized the singular value decomposition (SVD) algorithm to handle the high-dimensional ALFF data [31], resulting in 30 dimensions. Subsequently, we employed the K-means algorithm [32] to cluster MDD patients into distinct subtypes based on the 30-dimensional data. We tested cluster numbers ranging from K = 2 to K = 10, using the Dunn Index to evaluate the optimal K, where higher values indicate better clustering with more compact and well-separated clusters. These machine-learning algorithms were implemented using the scikit-learn library (version 0.22.2.post1) [33].

Measure of pro-inflammatory cytokines

Blood samples were collected from each participant via antecubital venipuncture between 8:00 AM and 12:00 PM on the day of the MRI scan. Immediately after collection, the samples were centrifuged at 3000 g for 5 min and stored at −80 °C until analysis.

Pro-inflammatory cytokine levels were measured from blood samples collected from participants. Levels of three common pro-inflammatory cytokines (TNF-alpha, IL-6, and IL-1 beta) were measured using the Human Premixed Multi-Analyte Kit (R&D Systems, Inc., Minneapolis, MN, United States) with the Human Magnetic Luminex Assay. Samples were magnetically labeled using a human, magnetic, premixed, microparticle cocktail of antibodies (Kit Lot Number L120614).

Multi-omics data acquisition

Peripheral blood samples were collected from participants for multi-omics profiling. Genomic, epigenomic, and metabolomic profiles were measured in this study. To obtain genomic data, we genotyped DNA samples following standard procedures, employing the Illumina Global Screening Chip-24 v1.0 BeadChip for Han Chinese populations. This BeadChip comprises 642,824 predetermined genetic variants and 53,411 custom-designed mutation sites. Epigenomic profiles were derived using the Illumina Infinium Methylation EPIC BeadChip [34], facilitating the quantitative analysis of over 850,000 methylation sites across the genome with single-nucleotide precision. For the metabolomic profile, untargeted metabolomics and lipid-omics analyses were conducted on the Ultimate 3000 Ultra Performance Liquid Chromatography coupled with the Q Interactive Quadrupole-Orbitrap High Resolution Mass Spectrometer (UPLC-HRMS) [35]. Detailed information could be checked in our prior publications [28, 36].

Calculation of epigenetic inflammation scores (EIS)

We utilized the ChAMP R package [37] to load the raw DNA methylation data, and filter probes and samples by default parameters (Supplementary Methods S2). Then the probes were normalized and corrected for technical batch effects and cell heterogeneity. All DNA methylation levels were expressed as β values, ranging from 0 to 1, calculated as M/(M+U), where

M is the signal from methylated beads, and U is the signal from unmethylated beads at the targeted CpG site.

The calculation of EIS is informed by methodologies established in prior research [38]. Specifically, we utilized findings from both the discovery and validation phases of a large-scale meta-analysis, involving 9 cohorts ($n = 8863$) and 4 cohorts ($n = 4111$) respectively, to select seven methylation sites significantly associated with plasma C-reactive protein (CRP) levels [38]. Due to the exclusion of one CpG site (cg06126421) from our dataset during quality control, our analysis proceeded with the six remaining CpG sites. The calculation involved multiplying the beta values of the six CpG sites by their respective regression weights and summing them to generate a composite score for each participant [39]. Given that all regression weights from the EWAS were negative, a lower EIS score is indicative of a higher state of inflammation, thus establishing a direct correlation between epigenetic markers and inflammation levels.

Estimation of epigenetic immune cell proportions

We utilized the reference-based GLINT method to assess the proportions of various immune cell types within each sample, relying on their methylation profiles [40]. This method estimates the proportion of monocytes, CD8+ cells, CD4+ cells, NK cells, B cells, neutrophils, and eosinophils according to the Houseman model, using a panel of 300 highly informative methylation sites in blood [41] and reference data collected from sorted blood cells [42]. It provides relative data of cell counts rather than absolute counts.

Identification of differential metabolites (DMs)

Following standard quality control procedures, a total of 669 metabolites were quantified. We applied linear regression modeling to identify the DMs associated with each subtype, incorporating 'group' as the independent variable and the relative abundance of each metabolite as the dependent variable, while adjusting for age, gender, BMI, and medication status as covariates. To account for multiple testing, we applied the Benjamini-Hochberg False Discovery Rate (FDR) correction, considering adjusted p values below 0.05 as statistically significant [43].

Calculation of polygenic risk scores (PRS)

Quality control of genomic data and imputation were performed before the calculation of PRS. The process included the exclusion of single nucleotide polymorphisms (SNPs) with a minor allele frequency (MAF) below 1%, a call rate less than 95%, or deviation from Hardy-Weinberg equilibrium (p value $< 10^{-5}$), and the exclusion of participants with more than 5% missing data, gender mismatches, or an identity-by-descent (IBD) score greater than 0.9. The refined genotype data were imputed using the GenoImpute engine [44]. The international MDD GWAS results published by the Psychiatric Genomics Consortium were used as discovery samples (https://pgc.unc.edu/), and our imputed genotyping data were used as a target sample. In the paper by the Major depressive disorder Working Group of the Psychiatric Genomics Consortium (PGC), the specific genetic factors contributing to MDD were analysed in 135,458 people with MDD and 344,901 controls [45]. PRSs were generated using PRSice software (www.PRSice.info). P-value-informed clumping was performed with a cut-off of $r^2 = 0.1$ in a 250 kb window. Seven PRSs at different p value thresholds (PT at 10^{-8}, 10^{-7}, 10^{-6}, 10^{-5}, 10^{-4}, 0.001, 0.01) were derived for each study participant.

Statistical analysis

We performed a descriptive analysis to evaluate the demographic and clinical characteristics of the participants. The normality of continuous variables was determined using the Shapiro-Wilk test. These variables are presented as means ± standard deviations (SD), while categorical data are expressed as frequencies and percentages. To investigate differences among subtypes, ANOVA analyses were conducted for continuous variables, and chi-square tests were utilized for categorical variables. In the evaluation of clinical measures, encompassing both clinical symptoms and cognitive performance, we employed ANOVA to assess statistical differences among the identified subtypes and HC. This was followed by post-hoc comparisons using Tukey's Honestly Significant Difference test to discern specific pairwise differences between the groups. A threshold of $p < 0.05$ was set to determine statistical significance.

To delineate the neuroimaging distinctions between subtypes and HC, we conducted a voxel-based two-sample t-test using the DPABI tool. Age and sex were included as covariates to mitigate potential biases, with statistical significance thresholds set at voxel p value of <0.001 and cluster p value of <0.05, corrected using the Gaussian random field (GRF) method.

Differences in pro-inflammatory cytokines, EIS, and proportions of seven immune cell types among the subtypes and HC were evaluated using ANOVA analysis respectively. To identify specific pairwise group differences, a post-hoc analysis was performed using Tukey's Honestly Significant Difference test. A p value of less than 0.05 was considered to denote a statistically significant difference.

Pearson correlation analysis was used to investigate associations between DMs and significantly differed pro-inflammatory cytokines.

The association of PRS-MDD with each subtype was investigated using logistic regression embedded in the software PRSice, adjusted for the first 20 principal components, age, and gender. Nagelkerke's pseudo-R^2 was calculated to measure the proportion of variance explained. To explore the biological pathways associated with these genetic variants, we conducted gene ontology (GO) enrichment analysis on the genes mapped to the significant PRS. This analysis, performed using the "clusterProfiler" package in R [46], covered three categories: cellular components (CC), molecular functions (MF), and biological processes (BP). To account for multiple testing, we applied the Benjamini-Hochberg FDR correction, considering p adjusted values below 0.05 as statistically significant [43]. We visually presented the top 10 significant pathways within each category to clearly represent the results.

Exploratory Pearson correlation analyses were conducted to examine the relationships among multi-omics measures, ALFF values, and clinical symptoms within each subtype. In Subtype 3, no significant alterations in multi-omics data were detected; therefore, we only performed correlations between ALFF values and clinical symptoms.

RESULTS

Characteristics of participants

Demographic and clinical characteristics of 327 MDD patients and 480 HC are presented in Table 1. There were significant differences between MDD patients and HC in age, gender, BMI, and education level. In clinical assessment, WCST scores (CC, CR, TE, PE, NPE), HAMD, and HAMA scores were significantly higher in MDD patients than in HC.

Identification of neuroimaging-based subtypes and their ALFF patterns

A total of 327 MDD patients were clustered into three subtypes based on ALFF data using the K-means algorithm, as determined by the Dunn Index (Fig. S1): Subtype 1 (28%), Subtype 2 (28%), and Subtype 3 (44%). Each subtype exhibited unique functional imbalance patterns in ALFF. In Subtype 1, ALFF was significantly elevated in limbic areas including the hippocampus, cingulate, amygdala, and thalamus, but notably decreased in the primary cortices such as the precentral cortex, occipital and postcentral cortex, in comparison to HC as depicted in (Fig. 1A). Subtype 2 showed a marked increase in ALFF within the prefrontal cortex and a decrease in the primary sensory cortices relative to HC (Fig. 1B). Conversely, Subtype 3 demonstrated a significant reduction in ALFF in the prefrontal cortex and an increase in the primary sensory cortices compared to HC (Fig. 1C). Detailed information about these region-specific alterations, aligned with the Automated Anatomical Labeling (AAL) atlas, is available in the Supplementary Table S1, S2, S3.

Demographic and clinical characteristics of the subtypes

In the comparison of demographic characteristics across the three identified subtypes and HC, significant differences were observed in gender, age, education and BMI level among the four groups (Table 1). The results of subsequent post-hoc analyses are presented in Table 1. Regarding clinical symptoms, post-hoc comparisons revealed that Subtype 1 had significantly higher HAMD scores than both Subtype 2 and Subtype 3. Subtype 1 also demonstrated more pronounced cognitive impairments in WCST than both Subtype 2 and Subtype 3. Specifically, Subtype 1 exhibited significantly lower CR scores and higher TE scores

Table 1. Demographic and clinical differences between MDD subtypes and HC.

	MDD patients ($N = 327$)	Health controls ($N = 480$)	p value[a] M-W U test	Subtype 1 ($N = 93$)	Subtype 2 ($N = 93$)	Subtype 3 ($N = 141$)	p value[b] ANOVA/$\chi 2$	F/$\chi 2$	Post hoc Turkey test
Demographics									
Gender, female (%)	67.9	59.8	0.02	73.1	55.9	72.3	<0.001	4.5	Subtype 3 > HC
Age, mean (S.D.), years	27.6 (10.6)	30.9 (11.8)	<0.001	30.4 (10.6)	24.3 (9.7)	27.9 (10.6)	0.004	10.6	Subtype 2 < Subtype 1, HC; Subtype 3 < HC
Education, mean (S.D.), years	12.3 (3.3)	14.1 (3.7)	<0.001	12.4 (3.2)	12.2 (2.9)	12.4 (3.6)	<0.001	15.5	Subtype 1, Subtype 2, Subtype 3 < HC
BMI, mean (S.D.)	21.9 (3.8)	22.6 (3.9)	0.02	21.7 (3.6)	22.9 (4.1)	21.5 (3.6)	0.009	3.9	Subtype 3 < Subtype 2, HC
Clinical characteristics									
Age of onset, mean (S.D.), years	24.9 (10.1)	—		27.9 (10.4)	22.7 (9.7)	24.9 (10.2)	0.009	4.7	Subtype 1 > Subtype 2
Duration, mean (S.D.), months	21.9 (41.8)	—		20.3 (31.4)	24.4 (36.1)	22.6 (51.1)	0.838	0.2	
Anti-depressants use									
Any (%)	23.5	0		47.3	63.4	61.0	0.050	3.0	
SSRI (%)	13.3	0		30.1	35.5	32.6	0.543	0.6	
TCA (%)	0	0		0	0	0	—	—	
MAO (%)	0	0		0	0	0	—	—	
Others (%)	17.6	0		36.6	44.1	47.5	0.484	0.7	
Clinical symptoms									
HAMD total score, mean (S.D.)	18.5 (9.9)	1.3 (2.3)	<0.001	21.1 (10.1)	18.1 (10.0)	17.4 (9.6)	<0.001	443.7	Subtype 1 > HC, Subtype 2, Subtype 3; Subtype 2, Subtype 3 > HC
HAMA total score, mean (S.D.)	16.3 (10.4)	1.2 (2.5)	<0.001	17.4 (10.3)	17.8 (10.2)	16.0 (11.1)	<0.001	293.5	Subtype 1, Subtype 2, Subtype 3 > HC
Cognition performance (WCST)	$N = 253$	$N = 383$		$N = 62$	$N = 76$	$N = 115$			
CR score of WCST, mean (S.D.)	28.5 (10.9)	30.2 (12.3)	0.008	24.9 (10.8)	30.0 (10.1)	29.4 (11.2)	0.013	3.6	Subtype 1 < Subtype 2
CC score of WCST, mean (S.D.)	3.6 (1.9)	3.9 (2.3)	0.052	3.2 (1.9)	3.9 (1.9)	3.7 (2.0)	0.099	2.1	
TE score of WCST, mean (S.D.)	19.5 (10.8)	17.8 (12.4)	0.01	23.1 (10.8)	17.9 (10.1)	18.6 (10.8)	0.012	3.7	Subtype 1 > Subtype 2
PE score of WCST, mean (S.D.)	7.1 (6.8)	6.4 (7.0)	0.014	9.4 (8.2)	6.5 (6.7)	6.3 (5.9)	0.013	3.6	Subtype 1 > Subtype 3
NPE score of WCST, mean (S.D.)	12.3 (6.7)	11.4 (7.2)	0.027	13.7 (6.3)	11.4 (5.9)	12.2 (7.2)	0.109	2.0	

Data are presented as either number (%) or means (standard deviations).
MDD major depressive disorder, *HC* healthy control, M-W U test Mann–Whitney U test, *SSRI* selective serotonin reuptake inhibitor, *TCA* tricyclic antidepressive, *MAO* monoamine oxidase inhibitor, *HAMD* hamilton depression scale, *HAMA* hamilton anxiety scale, *WCST* wisconsin card sorting test, *CR* correct responses, *CC* completed categories, *TE* total errors, *PE* perseverative errors, *NPE* non-perseverative errors.
[a]The examination between all MDD patients and the HC group.
[b]The examination of the three MDD subtypes and the HC group.

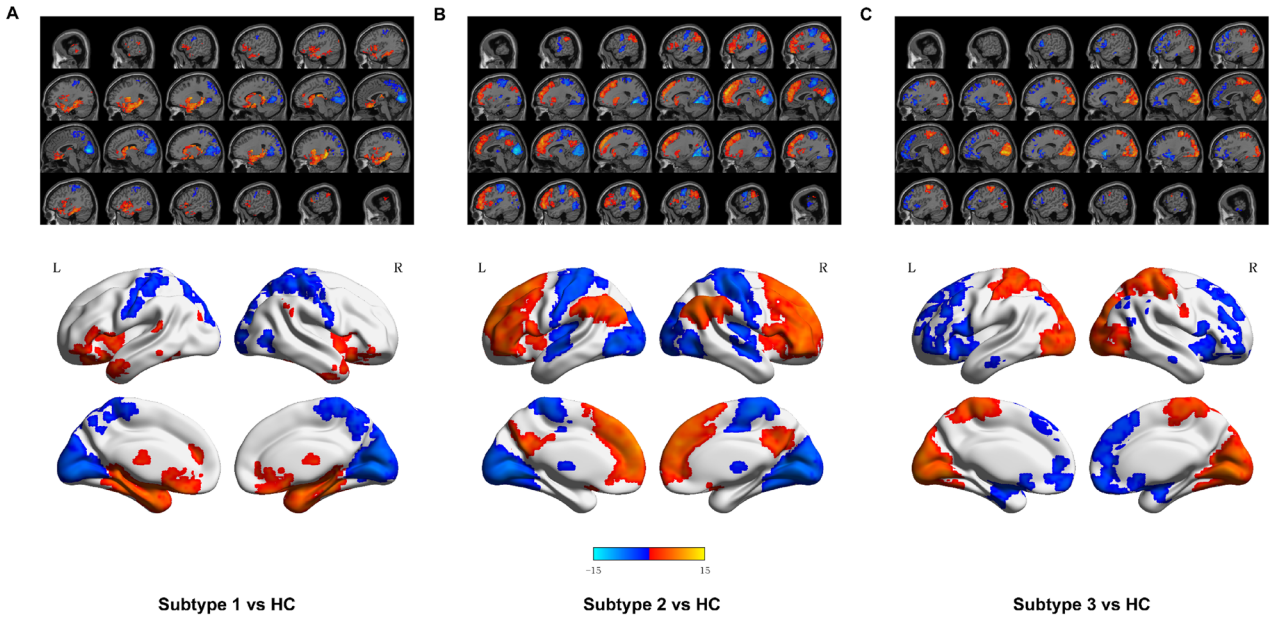

Fig. 1 Distinct functional alterations in three MDD subtypes. Brain charts display significantly differed brain regions in amplitude of low-frequency fluctuations (ALFF) in Subtype 1 **A**, Subtype 2 **B**, and Subtype 2 **C** compared to HC. The significance level was set to $p < 0.05$ (with Gaussian random field correction). L, left. R, right. The color bar represents the t-value. The elevated bar indicates a significant increase in ALFF of brain regions, and the lower bar indicates a significant decrease in ALFF in this subtype compared to HC. Red represents increased and blue decreased ALFF.

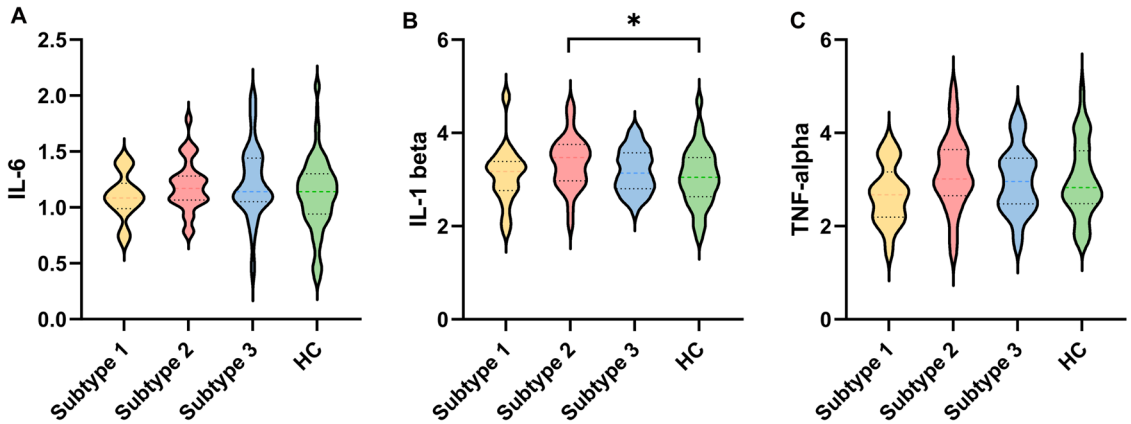

Fig. 2 Pro-inflammatory cytokines change in three MDD subtypes. Violin plots of the changes of IL-6 **A**, IL-1 beta **B**, and TNF-alpha **C** between each subtype and HC. *$p < 0.05$.

compared to Subtype 2. Subtype 1 had higher PE scores than Subtype 3. Detailed demographic and clinical statistical results are presented in Table 1.

Differences of Subtypes in molecular levels

Significant alteration of pro-inflammatory cytokine in Subtype 2. We compared the differences in pro-inflammatory cytokines among three subtypes and HC using ANOVA and post-hoc analysis. We found that IL-1 beta in Subtype 2 was more significantly elevated than HC (Fig. 2). TNF-alpha and IL-6 presented a trend of increased levels in Subtype 2, but did not reach statistical significance. This result indicated that Subtype 2 was in a higher inflammatory state than Subtype 1 and Subtype 3. Next, we further illuminate the inflammatory characteristics of Subtype 2 with multiple omics data.

Significant changes of inflammation indicators in methylation level underlying Subtype 2. EIS are refined indicators of chronic low-grade inflammation [47]. Distinct from traditional markers like plasma CRP levels, which are prone to significant variations in response to acute inflammatory stimuli, EIS provides a steadier reflection of chronic inflammation [48, 49]. The EIS, in particular, showcases enhanced test-retest reliability when compared to serum CRP levels, underscoring its value in offering a more reliable measure of inflammation's temporal stability [39]. Subtype 2 exhibited a significantly lower EIS compared to HC, indicating a higher state of inflammation (Fig. 3A). Subtype 1 and Subtype 3 did not show significant differences in EIS, as illustrated in Fig. 3A.

In the analysis of proportions of seven immune cell types derived from methylation data, Subtype 2 demonstrated a significantly higher proportion of neutrophils relative to HC, while the other six immune cell types showed no statistical significance (Fig. 3B–H). Subtype 1 and Subtype 3 did not show significant differences in the proportions of the seven immune cell types. Neutrophils are responsible for the first line of the host immune response against invading pathogens. They employ various mechanisms, including chemotaxis, phagocytosis, the release of reactive oxygen species (ROS) and granular proteins, and the

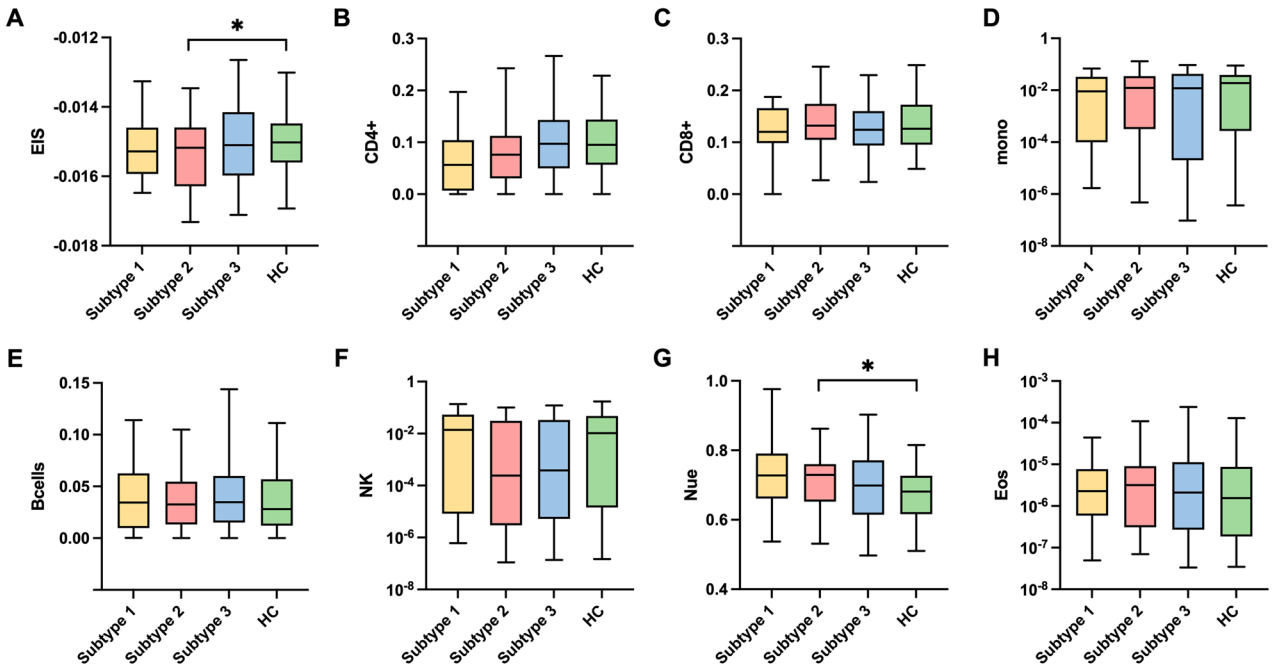

Fig. 3 Differences in epigenetic inflammation scores (EIS) and epigenetic immune cell proportions in three MDD subtypes. A The differences in EIS across three MDD subtypes and HC. **B**–**H** The differences in CD4+ **B**, CD8+ **C**, monocytes **D**, B cells **E**, NK cells **F**, neutrophils **G**, and eosinophils **H** cell proportions across three MDD subtypes and HC. A statistically significant distinction in EIS and neutrophil cell proportions was discerned between Subtype 2 and the HC. EIS, epigenetic inflammation score. *$p < 0.05$.

production and release of cytokines, all of which contribute to inflammation [50, 51]. These findings suggest that Subtype 2 is primarily associated with increased inflammation.

Significant metabolomic alterations and the correlation with IL-1 beta level underlying Subtype 2. In the analysis of DMs, we observed significant metabolic disturbances in Subtype 2. Compared to HC, Subtype 2 exhibited 36 DMs, while Subtype 1 and Subtype 3 did not show any DMs (Fig. 4A–C). In 36 DMs, 9 fatty acids, 8 triglycerides, 1 peptide, and 1 microbiome metabolite showed higher abundance, while 7 organic acids, 6 amino acids, 1 carbohydrate, and 3 unclassified metabolites showed decreased abundance in Subtype 2 compared to HC (Fig. 4D, E).

Pearson correlation analysis was used to further test the associations of DMs with IL-1 beta level, which was significantly higher in Subtype 2. 44% (16/36) of DMs significantly correlated with IL-1 beta levels in Subtype 2. Specifically, five of six amino acids: N-Acetylleucine, Acetyl-N-formyl-5-methoxykynurenamine, N-Acetylisoleucine, N-Lactoylvaline, and Methylglutaconic acid - were negatively correlated with plasma IL-1 beta. Similarly, six of the seven organic acids, including Fumaric acid, Isobutyric acid, Glutaric acid, Succinic acid semialdehyde, Dihydroxybutanoic acid, and Furoic acid, demonstrated significant negative associations with IL-1 beta (Fig. 4F).

Significant genetic predispositions underlying Subtype 1. PRS analysis revealed variation in genetic predispositions across the three MDD subtypes. Only Subtype 1 demonstrated significant genetic predisposition associated with MDD at PTs of 0.01 and 0.001 after adjusting for multiple comparisons (Fig. 5A). Subtype 2 and Subtype 3 did not exhibit a genetic liability related to MDD (Fig. 5B, C). Specifically, PRS-MDD at PT of 0.001 ($P = 0.011$, NSNPs = 1325) and 0.01 ($P = 0.002$, NSNPs = 4769) accounted for 5.9% and 8.1% of the phenotypic variance in Subtype 1, respectively. 4769 SNPs of PRS-MDD at the most significance threshold of PT = 0.01 were mapped to 2169 genes and found to be significantly enriched in pathways related to neuronal development and synaptic regulation. The top ten GO terms within each category were presented in Fig. 5D, mainly involved in 'synapse organization', 'regulation of neuron projection development', 'axonogenesis', 'postsynaptic membrane', 'neuron to neuron synapse', and 'monoatomic ion gated channel activity'. A complete list of all significant GO terms can be found in Supplementary Table S4, S5, and S6.

Association among multi-omics measures, ALFF values and clinical symptoms within each subtype. For Subtype 1, we performed Pearson correlation analyses among the PRS for MDD at four significance thresholds (PT = 0.01, 0.001, 10^{-5}, and 10^{-6}), ALFF values from nine significantly different clusters, and clinical symptoms. PRS-MDD at PT = 0.001 showed significant correlations with ALFF values in Cluster 4 (middle temporal gyrus) and Cluster 7 (supramarginal gyrus), as well as with HAMD factor scores. Additionally, ALFF values in Cluster 4 were significantly associated with both HAMD total and factor scores (Fig. 6A). For Subtype 2, correlation analyses were conducted between the significantly elevated pro-inflammatory cytokine IL-1 beta, ALFF values from the nine significant clusters, and clinical symptoms. IL-1 beta was significantly correlated with ALFF values in Cluster 2 (occipital gyrus) and HAMD factor scores. ALFF values in Cluster 8 precuneus were also significantly correlated with four indices from the WCST (Fig. 6B). For Subtype 3, we analyzed correlations between ALFF values from eleven significant clusters and clinical symptoms. ALFF values in Cluster 8 (postcentral gyrus) were significantly correlated with one WCST index, and ALFF values in Cluster 10 (angular gyrus) were significantly correlated with HAMD factor scores (Fig. 6C).

DISCUSSION

In this research, the utilization of machine learning clustering techniques on functional neuroimaging features (ALFF) in MDD patients identified three distinct subtypes—Subtype 1, Subtype 2, and Subtype 3. Each subtype was characterized by unique ALFF

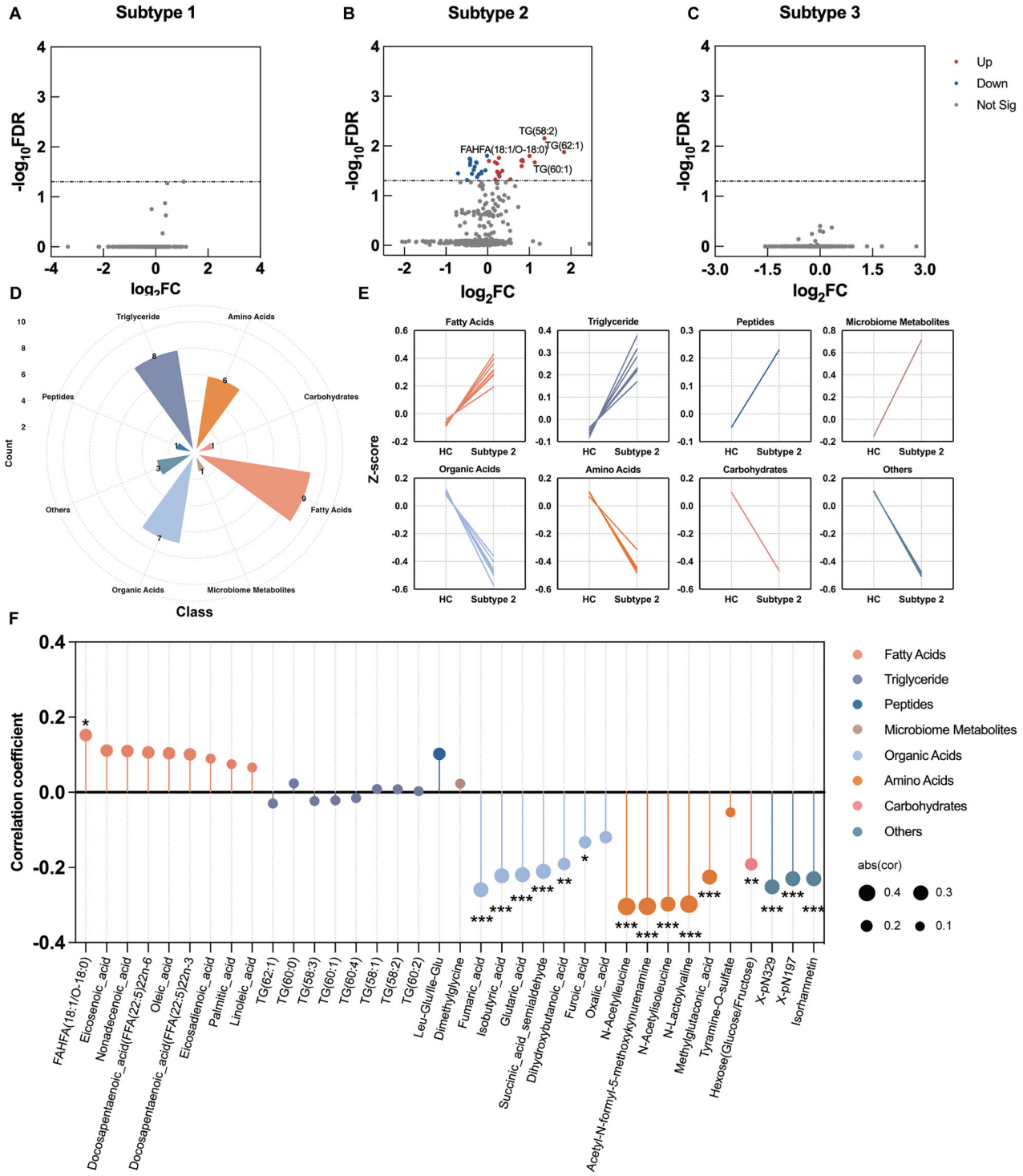

Fig. 4 Differential metabolites (DMs) in three MDD subtypes and their association with IL-1 beta. A–C Volcano plots of DMs related to MDD subtypes. **D** Nightingale Rose Chart of 8 DMs classes in Subtype 2, the different colors indicate different metabolite classes. **E** Line chart of DMs within 8 classes in Subtype 2 and HC groups. **F** Lollipop chart of the correlation coefficient between IL-1 beta and 36 DMs in Subtype 2. The x-axis denotes the 36 DMs in Subtype 2, and the y-axis represents the correlation coefficient. Calculated using Pearson correlation analysis. *$p < 0.05$ **$p < 0.01$ ***$p < 0.001$.

patterns. These distinctions were further substantiated through comprehensive multi-omics biological profiling, enriching our understanding of the specific etiological factors underlying each subtype. Subtype 1 features an imbalance of brain activity between the limbic system and primary cortices, with increased ALFF in the hippocampus, cingulate, and amygdala, and decreased ALFF in the primary visual, sensory, and motor cortices. This subtype indicates a strong genetic predisposition toward MDD, primarily enriched in neuronal development and synaptic regulation pathways, accompanied by severe depressive symptoms and cognitive decline. Subtype 2 reveals a different pattern of ALFF imbalance, with increased activity in the higher-order

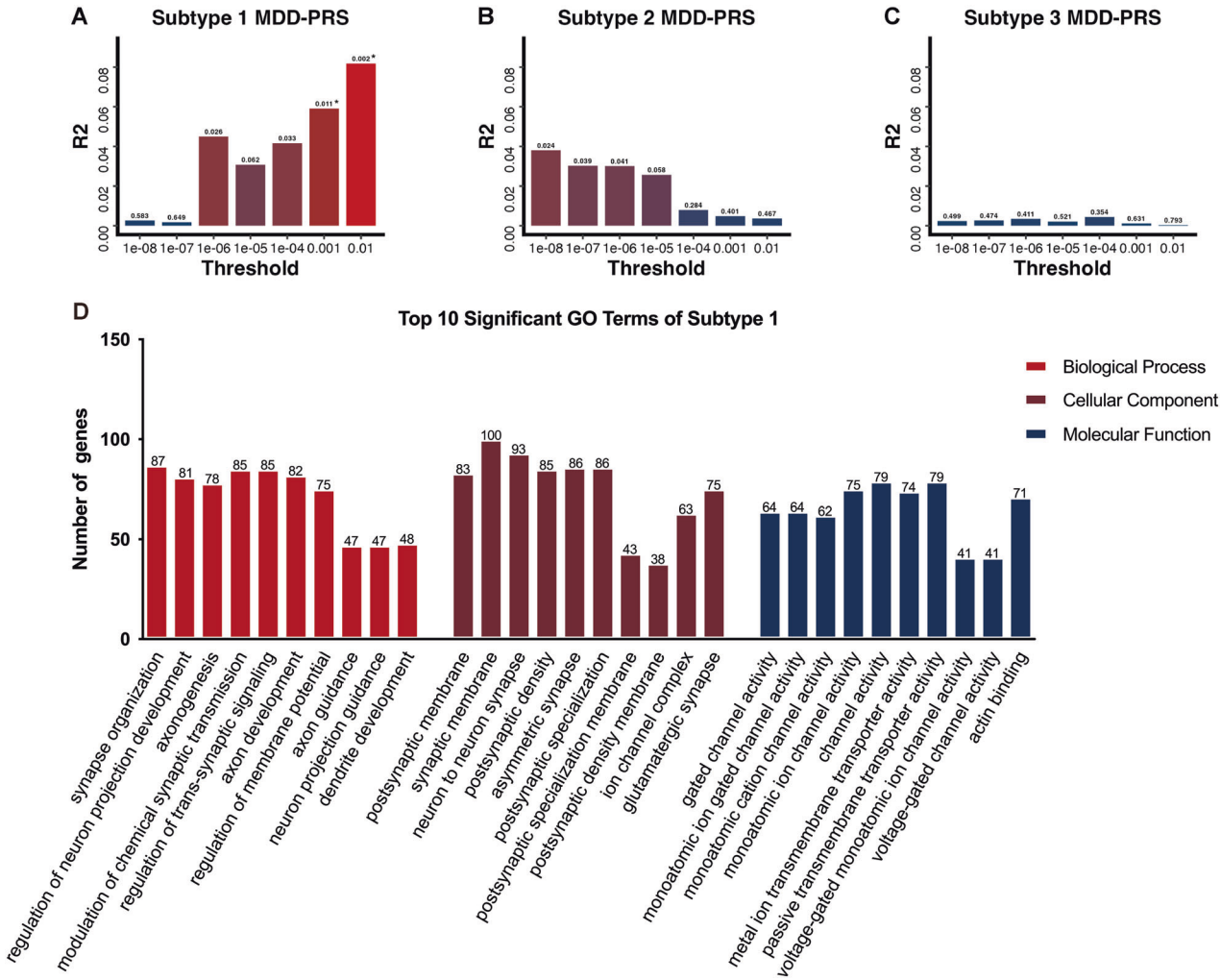

Fig. 5 Differences in genetic predispositions in three MDD subtypes. A–C Differential genetic predispositions of three MDD subtypes. The x-axis denotes the *p* value threshold, y-axis represents polygenic risk scores (PRS) model fit: R^2 (Nagelkerke's). The bars represent PRS calculated for MDD at seven different *p* value thresholds. * Indicates statistical significance with *p* adj < 0.05, corrected for FDR multiple comparisons. **D** Top 10 enriched GO categories for genes involved in the significant *p* value threshold (PT = 0.01).

cortices, notably the prefrontal cortex, and decreased activity in the primary cortices. Immune-inflammation dysregulation existed in Subtype 2, supported by multidimensional molecular evidence, including elevated IL-1 beta level, altered epigenetic inflammatory measures, and differential metabolites correlated with IL-1 beta level. Contrary to Subtype 2 in the ALFF pattern, Subtype 3 presents decreased activity in the prefrontal cortex and increased activity in primary cortices. There were no significant biological markers identified in Subtype 3. Our study showed that three subtypes may exhibit unique etiological mechanisms, with Subtype 1 predominantly influenced by genetic factors involved in neuronal development and synaptic regulation and Subtype 2 linked to immune-inflammatory processes. The variability of multidimensional features of subtypes reveals the complexity of MDD and highlights the potential of using neuroimaging-based subtypes to forge a path towards precision therapy in MDD.

Interestingly, all three subtypes demonstrate alterations in the primary sensory cortices, emphasizing their significance in MDD. Traditionally, the higher-order cortices and limbic system, known for their roles in cognitive and emotional regulation, have been the focus of the studies of neural mechanisms of MDD [52, 53]. The primary sensory cortices, tasked mainly with sensory input processing, have received less attention in MDD research. However, recent findings highlight the involvement of primary sensory cortices in higher-order functions, especially the visual cortex, suggesting its potential as a neuroregulatory target for alleviating depressive symptoms and improving cognitive function [54]. Our initial results from the MAM animal model, which revealed an imbalanced functional neuroimaging pattern between higher-order and primary cortices, showed that abnormal activity in the primary cortex has begun in adolescence, preceding abnormalities in the higher-order cortices that have appeared in early adulthood [55]. Studies by Jiang et al. on schizophrenia (SZ) patients examined the evolution of functional imaging features throughout the disease progression, revealing a gradual shift from the primary to higher-order cortices and subcortical areas as the disease advances [56]. These consistent observations indicate that changes in the primary cortex may be early indicators of psychiatric conditions like MDD and SZ, potentially making it a viable target for early intervention. Moreover, our prior animal study provided further support for these observations by demonstrating that targeted high-frequency repetitive Transcranial Magnetic Stimulation (rTMS) of the visual cortex during adolescence can reverse the abnormal functional connectivity in the higher-order cortex observed in early adulthood in a rat model of depression [57]. This outcome is further bolstered by human studies, where interventions targeting the visual cortex have proved effective for reversing abnormal

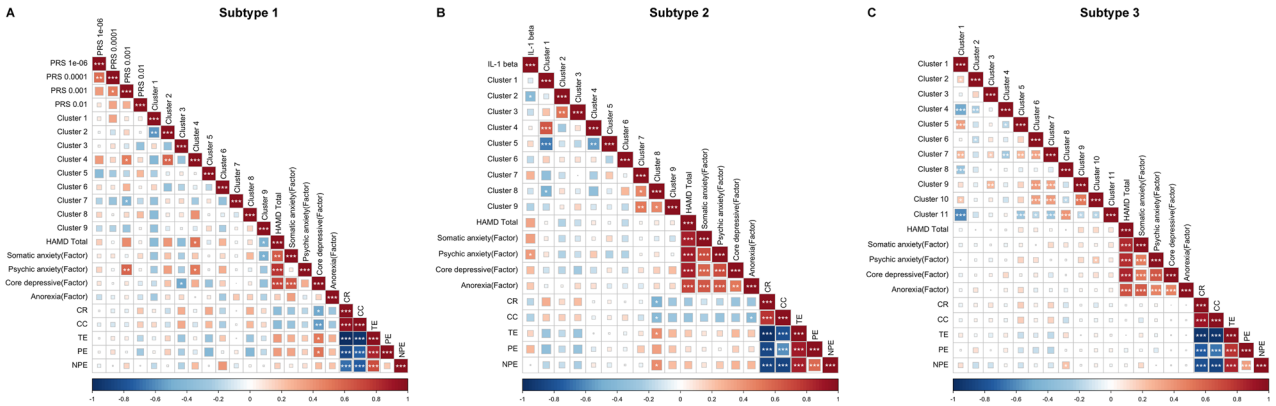

Fig. 6 Correlation between multi-omics, amplitude of low-frequency fluctuations (ALFF) values and clinical symptoms within each subtype. A Heatmap of Pearson correlation coefficients among polygenic risk scores (PRS), ALFF values and clinical symptoms within Subtype 1. **B** Heatmap of Pearson correlation coefficients among IL-1 beta, ALFF values and clinical symptoms within Subtype 2. **C** Heatmap of ALFF values and clinical symptoms within Subtype 3. The color bar indicates r-values, with red representing positive correlations and blue representing negative correlations. $*p < 0.05$ $**p < 0.01$ $***p < 0.001$.

neuroimaging and alleviating clinical symptoms [58] in mood disorders patients. Furthermore, one of our clinical trials showed that visual cortex stimulation significantly improved cognitive function in bipolar disorder (BD) patients [59]. These findings collectively suggest that primary cortices-targeted interventions may hold promising clinical utility.

The multi-omics evidence consistently indicates that immune-inflammatory dysregulation primarily drives the pathogenesis of Subtype 2. We observed a significant elevation of the pro-inflammatory cytokine IL-1 beta and pronounced metabolic dysregulation in Subtype 2 compared to HC. Notably, the disturbances in fatty acid, triglyceride, and amino acid metabolism were significantly correlated with IL-1 beta level. The association between immune-inflammatory damage and MDD has been robustly supported by human and animal research [60, 61]. Studies have identified increased levels of pro-inflammatory cytokines and acute response proteins in the plasma [62], central nervous system [63], and cerebrospinal fluid [64] of MDD patients, along with a rise in immune cells like neutrophils and monocytes [65, 66]. Clinical observations have shown that cytokine therapy, such as using IFN-α for chronic hepatitis, can lead to depressive-like behaviors, including anhedonia, anorexia, and reduced libido [67, 68]. Animal studies corroborate these findings, showing that inflammatory inducers like lipopolysaccharide (LPS) triggered depressive-like behaviors, such as decreased activity, appetite loss, and lowered sexual drive [69]. These findings suggest that at least a subset of MDD patients have immune-inflammatory damage.

Clinical trials have demonstrated promising evidence that anti-inflammatory treatments, both standalone and adjunct, can ameliorate depressive symptoms [70]. Targeted anti-inflammatory therapy, considering the biological heterogeneity of MDD, is especially crucial for patients with immune-inflammatory profiles. The challenge lies in accurately identifying this subgroup. Recent research has extended the use of molecular markers from cardiovascular to psychiatric domains, primarily utilizing molecular markers in peripheral blood for clinical stratification, such as CRP > 3 as an indicator of chronic inflammation [6]. These approaches offer valuable insights, yet the variability and potential somatic condition confounders of traditional peripheral inflammation markers hinder their clinical applicability. Neuroimaging features, serving as a conduit between peripheral inflammation and the central nervous system [71, 72], emerge as promising markers for identifying inflammatory subtypes in psychiatric disorders. In our study, distinct subtypes of MDD were identified based on ALFF, of which Subtype 2 was characterized by immune-inflammatory dysregulation and anti-inflammatory therapies would offer a promising adjunctive treatment modality for this subgroup.

Compared to Subtype 1 and Subtype 2, our multi-omics analysis did not definitively reveal the pathogenic mechanisms of Subtype 3, which shows neither significant genetic risk factors nor notable changes in inflammatory markers. We speculate that the etiology and pathological mechanisms of Subtype 3 are more complex and heterogeneous.

LIMITATION

Several limitations should be considered with regard to interpreting the current findings. Firstly, our whole-genome genetics and epigenetics data are limited in sample size, thus lacking the statistical power to identify specific genes or pathways associated with each subtype. This limitation prompted us to complement our analysis with large-sample-based validated results and summarized measures from whole-genome data, such as PRS and EIS, given the well-established understanding of MDD as a polygenic disorder. Secondly, not all MDD patients are medication-free, although there is no significant variation in medication use status among the three subtypes. Notably, medication does not influence the genetic profile. To address potential confounding effects, we included medication status as a covariate in our analysis of epigenetics and metabolomics data. Lastly, our study is cross-sectional, precluding the determination of direct causal effects of molecular alterations on each subtype. Future longitudinal studies are essential to explore the presence of causal relationships.

CONCLUSION

This study leveraged functional imaging to decipher the biological heterogeneity of MDD and employed multi-omics data to identify the primary biological mechanisms underlying the homogenous imaging subtypes: Subtype 1 is driven by genetic anomalies; Subtype 2 by immune-inflammatory dysregulation; and Subtype 3 by a complex mix. Our results offer a proof of concept for mechanism-targeted therapy in MDD.

DATA AVAILABILITY

The datasets used and/or analyzed during the current study are available from the corresponding author on reasonable request.

REFERENCES

1. Buch AM, Liston C. Dissecting diagnostic heterogeneity in depression by integrating neuroimaging and genetics. Neuropsychopharmacology. 2021;46:156–75.
2. Lynall M-E, McIntosh AM. The heterogeneity of depression. Am J Psychiatry. 2023;180:703–4.
3. Hasler G. Pathophysiology of depression: do we have any solid evidence of interest to clinicians? World Psychiatry. 2010;9:155–61.
4. Warden D, Rush AJ, Trivedi MH, Fava M, Wisniewski SR. The STAR*D Project results: a comprehensive review of findings. Curr Psychiatry Rep. 2007;9:449–59.
5. Rush AJ, Trivedi MH, Wisniewski SR, Nierenberg AA, Stewart JW, Warden D, et al. Acute and longer-term outcomes in depressed outpatients requiring one or several treatment steps: a STAR*D report. Am J Psychiatry. 2006;163:1905–17.
6. Drevets WC, Wittenberg GM, Bullmore ET, Manji HK. Immune targets for therapeutic development in depression: towards precision medicine. Nat Rev Drug Discov. 2022;21:224–44.
7. Kennard BD, Silva SG, Tonev S, Rohde P, Hughes JL, Vitiello B, et al. Remission and recovery in the treatment for adolescents with depression study (TADS): acute and long-term outcomes. J Am Acad Child Adolesc Psychiatry. 2009;48:186–95.
8. Drysdale AT, Grosenick L, Downar J, Dunlop K, Mansouri F, Meng Y, et al. Erratum: Resting-state connectivity biomarkers define neurophysiological subtypes of depression. Nat Med. 2017;23:264.
9. Lynch CJ, Gunning FM, Liston C. Causes and consequences of diagnostic heterogeneity in depression: paths to discovering novel biological depression subtypes. Biol Psychiatry. 2020;88:83–94.
10. Beijers L, Wardenaar KJ, van Loo HM, Schoevers RA. Data-driven biological subtypes of depression: systematic review of biological approaches to depression subtyping. Mol Psychiatry. 2019;24:888–900.
11. Zhang Y, Wu W, Toll RT, Naparstek S, Maron-Katz A, Watts M, et al. Identification of psychiatric disorder subtypes from functional connectivity patterns in resting-state electroencephalography. Nat Biomed Eng. 2021;5:309–23.
12. Fagiolini A, Kupfer DJ. Is treatment-resistant depression a unique subtype of depression? Biol Psychiatry. 2003;53:640–8.
13. Haroon E, Chen X, Li Z, Patel T, Woolwine BJ, Hu XP, et al. Increased inflammation and brain glutamate define a subtype of depression with decreased regional homogeneity, impaired network integrity, and anhedonia. Transl Psychiatry. 2018;8:189.
14. Nguyen TD, Harder A, Xiong Y, Kowalec K, Hägg S, Cai N, et al. Genetic heterogeneity and subtypes of major depression. Mol Psychiatry. 2022;27:1667–75.
15. Yu C, Arcos-Burgos M, Licinio J, Wong ML. A latent genetic subtype of major depression identified by whole-exome genotyping data in a Mexican-American cohort. Transl Psychiatry. 2017;7:e1134.
16. Meyer-Lindenberg A, Weinberger DR. Intermediate phenotypes and genetic mechanisms of psychiatric disorders. Nat Rev Neurosci. 2006;7:818–27.
17. Pearlson GD. Etiologic, phenomenologic, and endophenotypic overlap of schizophrenia and bipolar disorder. Annu Rev Clin Psychol. 2015;11:251–81.
18. Chen D, Wang X, Voon V, Jiang Y, Lo C-YZ, Wang L, et al. Neurophysiological stratification of major depressive disorder by distinct trajectories. Nat Ment Health. 2023;1:863–75.
19. Sun X, Sun J, Lu X, Dong Q, Zhang L, Wang W, et al. Mapping neurophysiological subtypes of major depressive disorder using normative models of the functional connectome. Biol Psychiatry. 2023;94:936–47.
20. Küblböck M, Woletz M, Höflich A, Sladky R, Kranz GS, Hoffmann A, et al. Stability of low-frequency fluctuation amplitudes in prolonged resting-state fMRI. Neuroimage. 2014;103:249–57.
21. Liu J, Ren L, Womer FY, Wang J, Fan G, Jiang W, et al. Alterations in amplitude of low frequency fluctuation in treatment-naïve major depressive disorder measured with resting-state fMRI. Hum Brain Mapp. 2014;35:4979–88.
22. Gong J, Wang J, Qiu S, Chen P, Luo Z, Wang J, et al. Common and distinct patterns of intrinsic brain activity alterations in major depression and bipolar disorder: voxel-based meta-analysis. Transl Psychiatry. 2020;10:353.
23. Teng C, Zhou J, Ma H, Tan Y, Wu X, Guan C, et al. Abnormal resting state activity of left middle occipital gyrus and its functional connectivity in female patients with major depressive disorder. BMC Psychiatry. 2018;18:370.
24. Meyer JH, Ginovart N, Boovariwala A, Sagrati S, Hussey D, Garcia A, et al. Elevated monoamine oxidase a levels in the brain: an explanation for the monoamine imbalance of major depression. Arch Gen Psychiatry. 2006;63:1209–16.
25. Kiecolt-Glaser JK, Derry HM, Fagundes CP. Inflammation: depression fans the flames and feasts on the heat. Am J Psychiatry. 2015;172:1075–91.
26. Scaini G, Mason BL, Diaz AP, Jha MK, Soares JC, Trivedi MH, et al. Dysregulation of mitochondrial dynamics, mitophagy and apoptosis in major depressive disorder: does inflammation play a role? Mol Psychiatry. 2022;27:1095–102.
27. Amin N, Liu J, Bonnechere B, MahmoudianDehkordi S, Arnold M, Batra R, et al. Interplay of metabolome and gut microbiome in individuals with major depressive disorder vs control individuals. JAMA Psychiatry. 2023;80:597–609.
28. Chang M, Womer FY, Gong X, Chen X, Tang L, Feng R, et al. Identifying and validating subtypes within major psychiatric disorders based on frontal-posterior functional imbalance via deep learning. Mol Psychiatry. 2021;26:2991–3002.
29. Guo H, Zhang R, Wang P, Zhang L, Yin Z, Zhang Y, et al. Brain functional and structural alterations in women with bipolar disorder and suicidality. Front Psychiatry. 2021;12:630849.
30. Duan J, Gong X, Womer FY, Sun K, Tang L, Liu J, et al. Neurodevelopmental trajectories, polygenic risk, and lipometabolism in vulnerability and resilience to schizophrenia. BMC Psychiatry. 2023;23:153.
31. Worsley KJ, Chen JI, Lerch J, Evans AC. Comparing functional connectivity via thresholding correlations and singular value decomposition. Philos Trans R Soc Lond B Biol Sci. 2005;360:913–20.
32. MacQueen J. Some methods for classification and analysis of multivariate observations. Fifth Berkeley Symposium on Mathematical Statistics and Probability. 1967;II:281–97.
33. Pedregosa F, Varoquaux G, Gramfort A, Michel V, Thirion B, Grisel O, et al. Scikit-learn:machine learning in python. J. Machine Learn. Res. 2011;12:2825–30.
34. Pidsley R, Zotenko E, Peters TJ, Lawrence MG, Risbridger GP, Molloy P, et al. Critical evaluation of the Illumina MethylationEPIC BeadChip microarray for whole-genome DNA methylation profiling. Genome Biol. 2016;17:208.
35. Khan N, Bano A, Rahman MA, Rathinasabapathi B, Babar MA. UPLC-HRMS-based untargeted metabolic profiling reveals changes in chickpea (Cicer arietinum) metabolome following long-term drought stress. Plant Cell Environ. 2019;42:115–32.
36. Zheng J, Womer FY, Tang L, Guo H, Zhang X, Tang Y, et al. Integrative omics analysis reveals epigenomic and transcriptomic signatures underlying brain structural deficits in major depressive disorder. Transl Psychiatry. 2024;14:17.
37. Tian Y, Morris TJ, Webster AP, Yang Z, Beck S, Feber A, et al. ChAMP: updated methylation analysis pipeline for Illumina BeadChips. Bioinformatics. 2017;33:3982–4.
38. Ligthart S, Marzi C, Aslibekyan S, Mendelson MM, Conneely KN, Tanaka T, et al. DNA methylation signatures of chronic low-grade inflammation are associated with complex diseases. Genome Biol. 2016;17:255.
39. Stevenson AJ, McCartney DL, Hillary RF, Campbell A, Morris SW, Bermingham ML, et al. Characterisation of an inflammation-related epigenetic score and its association with cognitive ability. Clin Epigenetics. 2020;12:113.
40. Rahmani E, Yedidim R, Shenhav L, Schweiger R, Weissbrod O, Zaitlen N, et al. GLINT: a user-friendly toolset for the analysis of high-throughput DNA-methylation array data. Bioinformatics. 2017;33:1870–2.
41. Koestler DC, Jones MJ, Usset J, Christensen BC, Butler RA, Kobor MS, et al. Improving cell mixture deconvolution by identifying optimal DNA methylation libraries (IDOL). BMC Bioinformatics. 2016;17:120.
42. Reinius LE, Acevedo N, Joerink M, Pershagen G, Dahlén SE, Greco D, et al. Differential DNA methylation in purified human blood cells: implications for cell lineage and studies on disease susceptibility. PLoS One. 2012;7:e41361.
43. Benjamini Y, Hochberg Y. Controlling the false discovery rate: a practical and powerful approach to multiple testing. J R Stat Soc Series B Stat Methodol. 2018;57:289–300.
44. Wang Y, Lu J, Yu J, Gibbs RA, Yu F. An integrative variant analysis pipeline for accurate genotype/haplotype inference in population NGS data. Genome Res. 2013;23:833–42.
45. Wray NR, Ripke S, Mattheisen M, Trzaskowski M, Byrne EM, Abdellaoui A, et al. Genome-wide association analyses identify 44 risk variants and refine the genetic architecture of major depression. Nat Genet. 2018;50:668–81.
46. Yu G, Wang LG, Han Y, He QY. clusterProfiler: an R package for comparing biological themes among gene clusters. OMICS. 2012;16:284–7.
47. Green C, Shen X, Stevenson AJ, Conole ELS, Harris MA, Barbu MC, et al. Structural brain correlates of serum and epigenetic markers of inflammation in major depressive disorder. Brain Behav Immun. 2021;92:39–48.
48. Barker ED, Cecil CAM, Walton E, Houtepen LC, O'Connor TG, Danese A, et al. Inflammation-related epigenetic risk and child and adolescent mental health: a prospective study from pregnancy to middle adolescence. Dev Psychopathol. 2018;30:1145–56.
49. Talens RP, Boomsma DI, Tobi EW, Kremer D, Jukema JW, Willemsen G, et al. Variation, patterns, and temporal stability of DNA methylation: considerations for epigenetic epidemiology. FASEB J. 2010;24:3135–44.
50. Pérez-Figueroa E, Álvarez-Carrasco P, Ortega E, Maldonado-Bernal C. Neutrophils: many ways to die. Front Immunol. 2021;12:631821.
51. Mantovani A, Cassatella MA, Costantini C, Jaillon S. Neutrophils in the activation and regulation of innate and adaptive immunity. Nat Rev Immunol. 2011;11:519–31.
52. Northoff G, Wiebking C, Feinberg T, Panksepp J. The 'resting-state hypothesis' of major depressive disorder-a translational subcortical-cortical framework for a system disorder. Neurosci Biobehav Rev. 2011;35:1929–45.

53. Phillips ML, Chase HW, Sheline YI, Etkin A, Almeida JR, Deckersbach T, et al. Identifying predictors, moderators, and mediators of antidepressant response in major depressive disorder: neuroimaging approaches. Am J Psychiatry. 2015;172:124–38.
54. Wu F, Lu Q, Kong Y, Zhang Z. A comprehensive overview of the role of visual cortex malfunction in depressive disorders: opportunities and challenges. Neurosci Bull. 2023;39:1426–38.
55. Sun D, Guo H, Womer FY, Yang J, Tang J, Liu J, et al. Frontal-posterior functional imbalance and aberrant function developmental patterns in schizophrenia. Transl Psychiatry. 2021;11:495.
56. Jiang S, Huang H, Zhou J, Li H, Duan M, Yao D, et al. Progressive trajectories of schizophrenia across symptoms, genes, and the brain. BMC Med. 2023;21:237.
57. Guo H, Xiao Y, Sun D, Yang J, Wang J, Wang H, et al. Early-stage repetitive transcranial magnetic stimulation altered posterior-anterior cerebrum effective connectivity in methylazoxymethanol acetate rats. Front Neurosci. 2021;15:652715.
58. Liu J, Guo H, Yang J, Xiao Y, Cai A, Zhao T, et al. Visual cortex repetitive transcranial magnetic stimulation (rTMS) reversing neurodevelopmental impairments in adolescents with major psychiatric disorders (MPDs): a cross-species translational study. CNS Neurosci Ther. 2024;30:e14427.
59. Wang D, Tang L, Xi C, Luo D, Liang Y, Huang Q, et al. Targeted visual cortex stimulation (TVCS): a novel neuro-navigated repetitive transcranial magnetic stimulation mode for improving cognitive function in bipolar disorder. Transl Psychiatry. 2023;13:193.
60. Berk M, Williams LJ, Jacka FN, O'Neil A, Pasco JA, Moylan S, et al. So depression is an inflammatory disease, but where does the inflammation come from? BMC Med. 2013;11:200.
61. Wohleb ES, Franklin T, Iwata M, Duman RS. Integrating neuroimmune systems in the neurobiology of depression. Nat Rev Neurosci. 2016;17:497–511.
62. Dowlati Y, Herrmann N, Swardfager W, Liu H, Sham L, Reim EK, et al. A meta-analysis of cytokines in major depression. Biol Psychiatry. 2010;67:446–57.
63. Kim YK, Na KS, Myint AM, Leonard BE. The role of pro-inflammatory cytokines in neuroinflammation, neurogenesis and the neuroendocrine system in major depression. Prog Neuropsychopharmacol Biol Psychiatry. 2016;64:277–84.
64. Enache D, Pariante CM, Mondelli V. Markers of central inflammation in major depressive disorder: a systematic review and meta-analysis of studies examining cerebrospinal fluid, positron emission tomography and post-mortem brain tissue. Brain Behav Immun. 2019;81:24–40.
65. Singh D, Guest PC, Dobrowolny H, Vasilevska V, Meyer-Lotz G, Bernstein HG, et al. Changes in leukocytes and CRP in different stages of major depression. J Neuroinflammation. 2022;19:74.
66. Sørensen NV, Frandsen BH, Orlovska-Waast S, Buus TB, Ødum N, Christensen RH, et al. Immune cell composition in unipolar depression: a comprehensive systematic review and meta-analysis. Mol Psychiatry. 2023;28:391–401.
67. Capuron L, Dantzer R. Cytokines and depression: the need for a new paradigm. Brain Behav Immun. 2003;17:S119–24.
68. Schaefer M, Schwaiger M, Garkisch AS, Pich M, Hinzpeter A, Uebelhack R, et al. Prevention of interferon-alpha associated depression in psychiatric risk patients with chronic hepatitis C. J Hepatol. 2005;42:793–8.
69. Dunn AJ, Swiergiel AH, de, Beaurepaire R. Cytokines as mediators of depression: what can we learn from animal studies? Neurosci Biobehav Rev. 2005;29:891–909.
70. Su WJ, Hu T, Jiang CL. Cool the inflamed brain: a novel anti-inflammatory strategy for the treatment of major depressive disorder. Curr Neuropharmacol. 2024;22:810–42.
71. Lin K, Shao R, Wang R, Lu W, Zou W, Chen K, et al. Inflammation, brain structure and cognition interrelations among individuals with differential risks for bipolar disorder. Brain Behav Immun. 2020;83:192–9.
72. Goldsmith DR, Bekhbat M, Mehta ND, Felger JC. Inflammation-related functional and structural dysconnectivity as a pathway to psychopathology. Biol Psychiatry. 2023;93:405–18.

ACKNOWLEDGEMENTS

We sincerely appreciate all the study participants for their patience and cooperation.

AUTHOR CONTRIBUTIONS

Conceptualization: Fei Wang, Lili Tang; methodology: Lili Tang; Xizhe Zhang; formal analysis: Lili Tang; resources: Yanqing Tang, Lili Tang, Rui Tang, Pengfei Zhao; investigation: Lili Tang, Rui Tang; writing – original draft preparation: Lili Tang, Rui Tang; writing – review and editing: Xiaohong Gong, Fei Wang; visualization: Lili Tang, Rui Tang; supervision: Fei Wang, Xizhe Zhang, Xiaohong Gong, Yanqing Tang; funding acquisition: Fei Wang, Xizhe Zhang, Rongxin Zhu, Junjie Zheng. All authors refined and approved the submitted version of the manuscript.

FUNDING

This work was supported by grants from NSFC-Guangdong Joint Fund [U20A6005 to Fei Wang], National Natural Science Foundation of China [62176129 to Xizhe Zhang], Jiangsu Provincial Key Research and Development Program [BE2021617 to Fei Wang], Strategic Topics Grant of University Grants Committee [STG1/M-501/23-N to Fei Wang], Jiangsu Provincial Medical Innovation Team, Key Project supported by Medical Science and Technology Development Foundation, Jiangsu Commission of Health [ZD2021026 to Rongxin Zhu], Jiangsu Provincial Key Research and Development Program [BE2022160 to Rongxin Zhu], Natural Science Foundation of Jiangsu Province [BK20231126 to Rongxin Zhu], China Postdoctoral Science Foundation [2022M721681 to Junjie Zheng]. We would like to thank all participants who took part in this study.

COMPETING INTERESTS

The authors declare no competing interests.

ADDITIONAL INFORMATION

Supplementary information The online version contains supplementary material available at https://doi.org/10.1038/s41398-025-03286-7.

Correspondence and requests for materials should be addressed to Yanqing Tang, Xizhe Zhang, Xiaohong Gong or Fei Wang.